

# Unibest-TC 2.0

Overview of model formulations

J. Bosboom, S.G.J. Aarninkhof,  
A.J.H.M. Reniers, J.A. Roelvink,  
D.J.R. Walstra

January, 2000

---

## Contents

<b>1 Introduction</b> .....	<b>1-1</b>
<b>2 Overview of sub-models</b> .....	<b>2-1</b>
<b>3 Wave model</b> .....	<b>3-1</b>
<b>4 Mean current profile</b> .....	<b>4-1</b>
4.1 Introduction .....	4-1
4.2 Momentum balance .....	4-2
4.3 Vertical structure of eddy viscosity.....	4-4
4.4 Integration of velocity profile .....	4-5
4.5 Specification of eddy viscosity distribution.....	4-7
<b>5 Near-bed orbital velocity</b> .....	<b>5-1</b>
<b>6 Bed load transport</b> .....	<b>6-1</b>
6.1 General .....	6-1
6.2 Bed-load transport formulation.....	6-1
<b>7 Suspended load transport</b> .....	<b>7-1</b>
7.1 General .....	7-1
7.2 Suspended load transport formulation .....	7-2
<b>8 Time averaged concentration profile</b> .....	<b>8-1</b>
8.1 Convection-diffusion equation.....	8-1
8.2 Sediment fall velocity and turbulence damping.....	8-1
8.3 Sediment mixing coefficient .....	8-2
8.4 Reference concentration near the bed.....	8-5
<b>9 Bed shear stress formulations</b> .....	<b>9-6</b>
9.1 Introduction.....	9-6
9.2 General procedure for the bed shear stress .....	9-6

9.3 Bed shear stress in suspended load model .....	9-5
9.4 Bed shear stress in bed load model .....	9-6

## Acknowledgements

This review of the formulations in the cross-shore profile model UNIBEST-TC has been undertaken as part of the MAST3 SAFE research project. It was partly funded by the Commission of the European Communities, Directorate General for Science, Research and Development, under contractno. MAS3-CT95-0004.

# I Introduction

## Background

In a study for “Rijkswaterstaat” RIKZ (Van Rijn et al., 1995) to predict the yearly averaged cross-shore and longshore sediment transport rates for several cross-shore profiles along the closed part of the Dutch coast, the predictions obtained at the 20 and 8 m depth contour differ considerably from the results obtained for a similar study carried out in 1989. The latter study was based on the Bailard-Bagnold transport formulation, whereas the newly performed sediment transport computations were obtained by implementing state of the art knowledge on hydrodynamics and morphology.

Based on this study, it was decided to upgrade the formulations in the UNIBEST-TC model to the same level as the model used to evaluate the yearly averaged sediment transports at the 20 and 8 m water depth. Besides, the wave energy decay model has been modified according to Roelvink et al. (1995).

The upgraded model (version 2.0) as described in DELFT HYDRAULICS (1995) and the present report differs from the previous version (version 1.0) in the following respects:

- a new sediment transport formulation according to Van Rijn et al. (1995). In this formulation, bed load and suspended load are treated in fundamentally different ways.
- a consistent treatment of the cross-shore and longshore velocity vertical, using parametric viscosity distributions.
- the inclusion of wind-driven currents
- inclusion of the surface roller contribution in the momentum balance
- inclusion of breaker delay in wave energy decay model

In the Bailard formula, used in the previous versions, bed load and suspended load were assumed to react instantaneously to velocity fluctuations. This is probably correct for bed load but certainly not for suspended load. In the upgraded model, the suspended sediment flux is approximated by the product of mean current and mean concentration verticals. It is now possible that bed load and suspended load transport are in opposite directions. In the surf zone, the bed load transport will generally be directed onshore and the suspended transport offshore. In previous versions of the model, the suspended transport was mainly directed onshore, which led to unrealistic accretion of the upper profile.

The modelling of the mean current has been improved, resulting in a consistent treatment of the cross-shore and longshore velocity vertical. In the momentum equations and the parametric viscosity distributions, account is taken of wind shear stress, wave breaking, dissipation in the wave boundary layer and the slope of the free surface.

Investigation of model performance learned that model predictions of wave height decay were reasonably well in correspondance with wave height measurement through the surf zone,

however, the location of initial set-up was predicted too far seaward. For that reason the roller model according to Nairn et al. (1990) has been incorporated in UNIBEST-TC. Instead of being dissipated immediately after the breakpoint, organized wave energy is converted into turbulent kinetic energy first (which can be seen from the development of a roller at the face of a breaking wave), before being dissipated ultimately via the production of turbulence. In this way the dissipation process is delayed, hence shifting the region of wave set-up in shoreward direction.

It has often been noticed, and most recently during the validation of UNIBEST-TC against the LIP-11D Deltaflume tests, that the process of wave breaking is not accurately described by the Battjes and Janssen model, used in UNIBEST-TC, in the case of rather strong bottom variations. The sub-model which predicts the fraction of breaking waves reacts only to the water depth and disregards the fact that waves need a distance in the order of one wave length to respond and actually start or stop breaking. The inclusion of this so-called breaker delay in the wave energy decay model of version 2.0 was found to significantly improve the predictions of bar behaviour.

The upgraded model has been validated (Reniers et al., 1995) against the data obtained during the LIP-11D Deltaflume tests performed in spring 1993. In subsequent applications of the upgraded model, it was found that the new formulations result in fundamental improvements of the morphodynamic behaviour

The aim of this report is to give a complete overview of the model formulations presently applied in the cross-shore profile model UNIBEST-TC (version 2.0). The model formulations itself do not differ from the upgraded formulations as described in DELFT HYDRAULICS (1995), but are dealt with in more detail in the present report.

## **Outline of report**

In Chapter 2, an overview is given of the various sub-models in UNIBEST-TC. Subsequently, Chapter 3 gives the equations underlying the wave propagation model. The mean current profile and near-bed orbital velocity models are presented in Chapters 4 and 5 respectively.

The formulations for bed load and suspended load transport are described in Chapters 7 and 8, respectively. The computation of the time-averaged concentration profile, which is needed in the suspended load model is discussed in Chapter 8. For the bed shear stress, slightly different formulations are applied in the in the bed load and suspended load transport modules, respectively. These formulations for the bed shear stress are dealt with in Chapter 9.

## **Coordinate system**

The x-axis is perpendicular to the shoreline, positive landwards. The y-axis is rotated 90 degrees counter-clockwise, relative to the x-axis. The z-axis is perpendicular to the x- and y-axis, positive in upward direction. Wave angles are defined between the x-axis and the direction of wave propagation, positive angles counting counter-clockwise.

## 2 Overview of sub-models

The UNIBEST-TC model consists of five sub-models:

- wave propagation model
- mean current profile model
- wave orbital velocity model
- bed load and suspended load transport model
- bed level change model

A schematic representation of the various sub-models is given in Figure 2.1.

The wave propagation model computes the wave energy decay along a cross-shore ray including the effects of shoaling, refraction and energy dissipation. The mean current profile model as well as the wave orbital velocity model are local models. The first computes the vertical distribution of the wave-averaged mean current in both longshore and cross-shore direction accounting for wind shear stress, wave breaking, bottom dissipation in the wave boundary layer and the slope of the free surface. The wave orbital velocity model calculates time series of the near-bed wave orbital velocity. These time series contain contributions due to wave asymmetry, wave group related amplitude modulation and bound long waves and are therefore representative for irregular wave groups.

In the sediment transport model one can distinguish between the bed load and suspended load module respectively. It is assumed that the suspended load transport is dominated by the transport by the mean current; the suspended sediment flux is computed as the product of the wave-averaged current and concentration profiles, which are obtained from the mean current profile model and a time-averaged advection-diffusion equation respectively. The bed-load transport is computed as a function of the instantaneous bed shear stress. The near-bed velocity signals, determining the instantaneous bed shear stresses, are composed of the generated time-series for the near-bed wave orbital velocity plus the time-averaged current velocity near the bed.

After the computation of the transport rates along the profile, the bed level changes are computed from the depth-integrated mass balance:

$$\frac{\partial z}{\partial t} + \frac{\partial q_{bot+sus}}{\partial x} = 0$$

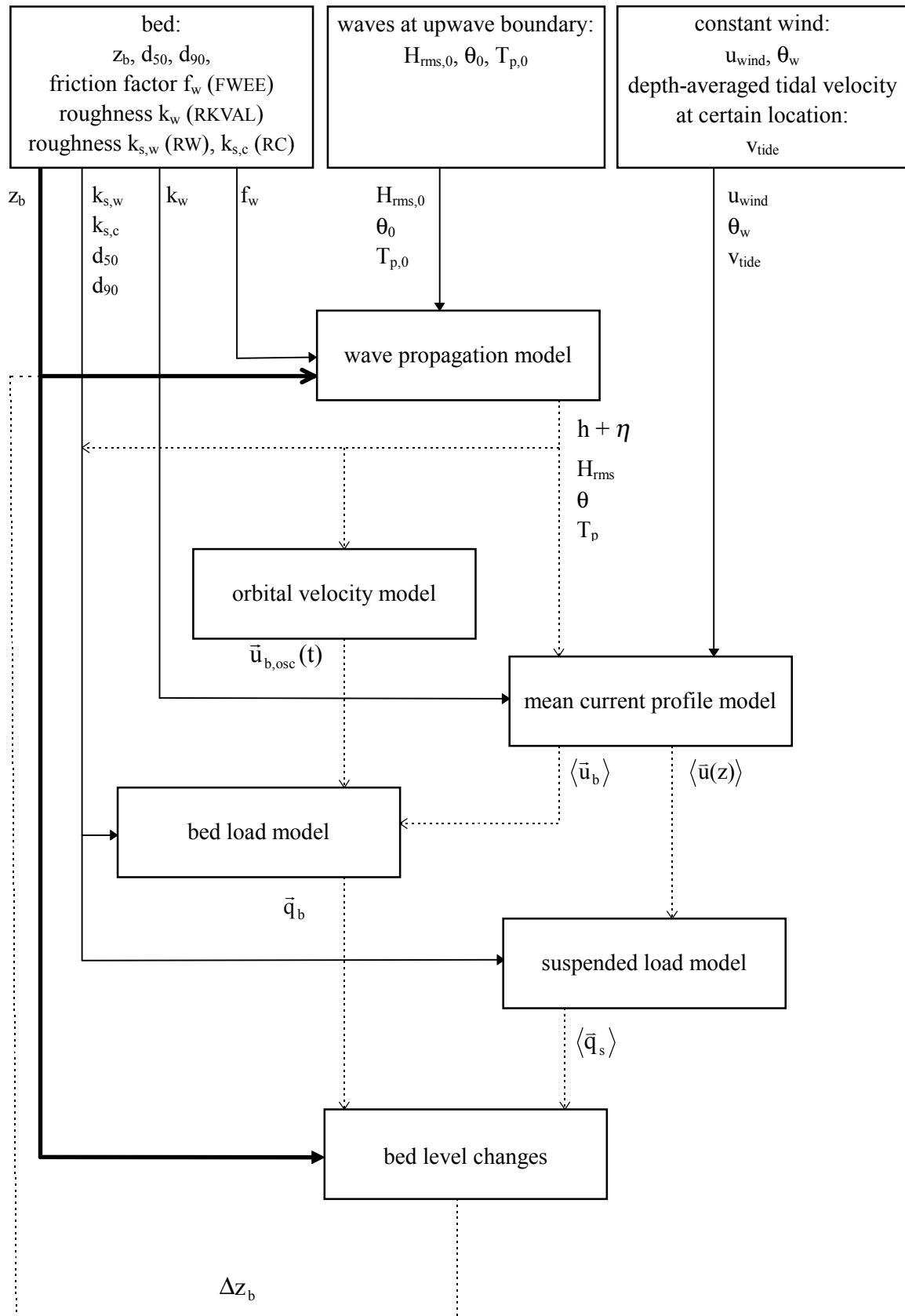


Figure 2.1 Overview of UNIBEST-TC sub-models (text in small capitals corresponds to the names in the input file)

### 3 Wave model

The wave propagation model consists of three first-order differential equations, viz. the time-averaged wave energy balance (Battjes and Janssen, 1978), the balance equation for the energy contained in surface rollers in breaking waves (Nairn et al., 1990) and the horizontal momentum balance from which the mean water level set-up is computed. The refraction of the waves is computed using Snell's law. The three coupled equations are solved by numerical integration over the cross-shore profile. These equations generate the input required by the local models for the vertical velocity profile, the concentration vertical and the bed-load transport.

The energy balance equation for organised wave energy  $E$  reads:

$$\frac{\partial}{\partial x}(EC_g \cos \theta) = -D_w - D_f \quad (3.1)$$

where  $C_g$  is the wave group velocity,  $\theta$  the angle of incidence of the wave field,  $D_w$  the dissipation of wave energy due to breaking and  $D_f$  the dissipation due to bottom friction. The organised wave energy  $E$  is defined according to linear wave theory

$$E = \frac{1}{8} \rho g H_{rms}^2 \quad (3.2)$$

where  $\rho$  is the density of water,  $g$  the gravitational acceleration and  $H_{rms}$  the root mean square wave height.

Battjes and Janssen use as a closure for this an expression for the dissipation of organised wave energy based on a bore model:

$$D_w = \frac{1}{4} \rho g \alpha f_p H_{max}^2 Q_b \quad (3.3)$$

where  $f_p = 1/T_p$  is the peak frequency,  $Q_b$  the fraction of breaking waves and  $\alpha$  a dissipation coefficient, which equals 1 in case of a fully developed bore. The model applies a so-called clipped Rayleigh through the surf zone, assuming that the waves smaller than  $H_{max}$  are not breaking and Rayleigh distributed, and that all waves larger than  $H_{max}$  are breaking. This maximum wave height  $H_{max}$  is defined as a function of the local water depth, according to:

$$H_{max} = \frac{0.88}{k} \tanh\left(\frac{\gamma k h_r}{0.88}\right) \quad (3.4)$$

where  $k$  is the local wave number,  $h_r$  the local waterdepth (which was modified later on by Roelvink et al. (1995), see Eq. .11) and  $\gamma$  a dissipation coefficient. Battjes and Stive (1985) performed an extensive calibration study for  $\gamma$ , based on both field and laboratory data.

Setting  $\alpha$  equal to 1, the best fit values for  $\gamma$  turned out to vary systematically with the offshore wave steepness  $s_0 = H_{rms,0}/L_0$ , according to

$$\gamma = 0.5 + 0.4 \tanh(33s_0) \quad (3.5)$$

Equation 3.5 expresses the default relationship for  $\gamma$  as applied by UNIBEST-TC. The fraction of breaking waves  $Q_b$  reflects the percentage of waves larger than  $H_{max}$  and is computed iteratively from

$$\begin{aligned} \frac{1 - Q_b}{\ln(Q_b)} &= - \left( \frac{H_{rms}}{H_{max}} \right)^2 && \text{for } \frac{H_{rms}}{H_{max}} < 1 \\ Q_b &= \left( \frac{H_{rms}}{H_{max}} \right)^2 && \text{for } \frac{H_{rms}}{H_{max}} \geq 1 \end{aligned} \quad (3.6)$$

Though ‘impossible’ from a theoretical point of view, it may occur that the value of  $H_{rms}$  exceeds the value of  $H_{max}$  in very shallow water (frequently in combination with plunging breakers). In those situations the second formulation of Eq. 3.6 is applied, which in fact implies that the maximum wave height  $H_{max}$  in Eq. 3.3 is replaced by the local wave height  $H_{rms}$ , hence introducing extra wave dissipation in a region where  $H_{rms}$  actually is too large. Finally, the wave dissipation  $D_f$  due to bottom friction, which is the second sink term in Eq. 3.1, is modelled as

$$D_f = \frac{f_w \rho}{\sqrt{\pi}} u_{orb}^3 \quad (3.7)$$

where  $f_w$  is a user defined friction factor (FWEE) and  $u_{orb}$  the amplitude of the wave orbital velocity based on linear wave theory and the rms wave height.

Investigation of model performance learned that model predictions of wave height decay were reasonably well in correspondance with wave height measurement through the surf zone, however, the location of initial set-up was predicted too far seaward. For that reason the roller model according to Nairn et al. (1990) has been incorporated in UNIBEST-TC. Instead of being dissipated immediately after the breakpoint, organized wave energy is converted into turbulent kinetic energy first (which can be seen from the development of a roller at the face of a breaking wave), before being dissipated ultimately via the production of turbulence. In this way the dissipation process is delayed, hence shifting the region of wave set-up in shoreward direction. This roller model provides the second differential equation of the UNIBEST model, the roller balance equation:

$$\frac{\partial}{\partial x} (2E_r C \cos \theta) = D_w - Diss \quad (3.8)$$

In this expression,  $c$  is the wave propagation speed,  $Diss$  the dissipation of roller energy and  $D_w$  the dissipation of organised wave energy which acts as a source term for the roller balance equation. The factor ‘2’ in Eq. 3.8 originates from additional dissipation of roller

energy due to a net transfer of water from the wave to the roller (Stive and De Vriend, 1994). The roller energy  $E_r$  represents the amount of kinetic energy in a roller with area  $A$  and length  $L$ , and is defined as

$$E_r = \frac{1}{2} \rho c^2 \frac{A}{L} \quad (3.9)$$

The roller energy balance is closed by modelling the dissipation  $Diss$  of roller energy as the power per unit length performed by the shear stress between roller and water surface:

$$Diss = \beta \rho g c \frac{A}{L} = 2\beta g \frac{E_r}{C} \quad (3.10)$$

where  $\beta$  is the slope of the face of the wave (normally in the range 0.05-0.10) and  $A$  is written in terms of  $E_r$  via Eq. 3.9.

In order to improve the prediction of bar morphodynamics, Roelvink et al. (1995) introduced their concept of breaker delay. The dissipation of organised wave energy as computed from Eq. 3.3 and 3.4 is only based on local water depth, and disregards the fact that waves need a distance in the order of one wave length to actually start or stop breaking. For that reason they suggest to take into account the bottom elevation some distance seaward of the computational point when determining the water depth  $h_r$  to be applied in Eq. 3.4. To that end they define a reference depth  $h_r$ , obtained from weighting water depths seaward of the computational point via a weighing function  $W(\xi)$ :

$$h_r(x) = \frac{\int_{x-X}^x W(x-x') h(x') dx'}{\int_{x-X}^x W(x-x') dx'} \quad (3.11)$$

In this expression,  $h$  is the local water depth and  $X$  is the integration distance. The weighting function  $W$  is given by:

$$W(\xi) = (X - \xi)^p \quad (3.12)$$

where  $p$  is a user defined parameter which determines the shape of the weighting function. The integration distance  $X$  is taken proportional to the local peak wave length  $L_p$ :

$$X = \lambda L_p \quad (3.13)$$

where  $\lambda$  is a user defined coefficient of order one.

The third differential equation is the cross-shore momentum equation or set-up equation, which reads:

$$\frac{\partial \bar{\eta}}{\partial x} = -\frac{1}{\rho g h} \frac{\partial S_{xx}}{\partial x} \quad (3.14)$$

Here,  $\bar{\eta}$  is the mean wave set-up,  $h = \bar{\eta} - z_b$  the local water depth  $h$  and  $S_{xx}$  the cross-shore radiation stress, which is defined as

$$S_{xx} = \left( (n + n \cos^2 \theta - 0.5)E + 2E_r \cos^2 \theta \right) \quad (3.15)$$

where  $n = C_g/C$ , the ratio between wave propagation speed and the group velocity. The wave direction  $\theta$  is defined as the angle between the  $x$ -axis (perpendicular to the shoreline, positive landwards) and the propagation direction, and is found from Snell's law:

$$\frac{\sin \theta}{\sin \theta_0} = \frac{C}{C_0} \quad (3.16)$$

where the subscript  $0$  refers to values at the seaward boundary of the model.

Finally the propagation speed  $C$  is defined as

$$C = \omega / k \quad (3.17)$$

where  $\omega = 2\pi f_p$  is the angular frequency, and  $k$  is the wave number, which is solved from the dispersion relation:

$$\omega^2 = gk \tanh(kh) \quad (3.18)$$

In order to solve the system for the three unknown  $E$ ,  $E_r$  and  $\eta$ , boundary conditions for  $E$ ,  $E_r$ ,  $\eta$  and  $\theta$  and a bottom profile  $z_b(x)$  are needed; The boundary value of  $E$  is computed from Eq. 3.2 via a user defined wave height at the upwave boundary. In addition,  $\theta$  and  $z_b(x)$  should given at the upwave boundary, while  $\eta$  is set to zero which is reasonable if the upwave boundary is located outside the surf zone. The roller energy  $E_r$  at the seaward boundary is estimated from Eq. 3.10, assuming that  $D_{iss}$  equals  $D_w$ . Coefficient values must be given for  $\alpha$  (default value 1),  $\gamma$  (default value given by Eq. 3.5),  $\beta$  (optimum value between 0.05 and 0.10) and  $\lambda$  (value of order 1)

## 4 Mean current profile

### 4.1 Introduction

In an alongshore uniform situation, the depth-integrated cross-shore radiation stress balances the wave-set up. The longshore radiation stress gradient on the other hand, is balanced by a time mean bed shear stress associated with a longshore current. Due to the vertical non-uniformity of the driving forces in the nearshore zone, secondary currents are driven. The imbalance between the cross-shore wave radiation stress gradient (with contributions due to wave height decay and change of momentum in surface rollers) and the pressure gradient due to the set-up, drives a circulation current with a shoreward mass flux above the trough level and a seaward return flow or undertow below trough level. Besides, due to wave boundary layer effects in the momentum balance, a near-bottom streaming in the wave boundary layer occurs, which is often assumed to be shoreward directed.

In order to determine the velocity distribution of the cross-shore circulation current and the longshore current, the horizontal momentum balance needs to be solved. This is done according to Roelvink and Reniers (1994) who use a quasi-3D model in which account is taken of the effects of wind stress, breaking-induced forcing, surface slope and the wave boundary layer. A parabolic distribution of the eddy viscosity is used in which the effects of turbulence from different sources (slope-driven and wind-driven current, wave breaking and increased turbulence in the wave boundary layer) are combined in a consistent manner.

The quasi-3D model is a direct descendant of the model according to De Vriend and Stive (1987) who identify three layers:

- the surface or trough-to-crest layer, which is represented by boundary conditions on the middle layer;
- the middle layer, from the top of the bottom (wave) boundary layer to the mean water level;
- the bottom boundary layer.

Svendsen (1985) and Stive and de Wind (1986) were the first to propose only to consider the area below wave trough level and account for the trough-to-crest layer, containing the moving water surface, via an effective shear stress at the trough level, compensating for the momentum decay above it, and via the condition that the net mean flow below trough level must compensate for the mass flux in the surface layer. The modelling of the surface layer is thus reduced to the formulation of the effective shear stress and the mass flux. For simplicity, here we use the mean water level as the upper boundary of the middle layer.

In the following sections, the momentum balance and required turbulence closure (eddy viscosity model) are described. First, Section 4.2 deals with the momentum balance, whereafter in Section 4.3 the shape of the eddy viscosity distribution is described. Using the latter eddy viscosity distribution, the equations can be integrated analytically yielding

formulations for the depth-averaged velocity and the velocity vertical as described in Section 4.4. Finally, in Section 4.5 the parameters necessary to fully define the eddy viscosity distribution are specified.

## 4.2 Momentum balance

For simplicity, the vertical coordinate is scaled according to:

$$\sigma = \frac{z}{h}, \quad (4.1)$$

such that  $\sigma = 0$  at the bottom and 1 at the surface

Neglecting the advective acceleration terms for the time mean flow, the momentum balance in  $i$ -direction,  $i = x$  or  $y$ , reads:

$$\frac{\partial \tau_i}{\partial \sigma} = R_i, \quad , \sigma > \delta \quad (4.2a)$$

$$\frac{\partial \tau_i}{\partial \sigma} = R_i + \frac{\partial}{\partial \sigma}(\rho \tilde{u}_i \tilde{w}) \quad , \sigma < \delta \quad (4.2b)$$

where  $R_i$  is the forcing,  $\delta$  the *non-dimensional* thickness of the wave boundary layer made dimensionless according to Eq. (4.1), and  $\tilde{u}_i$  and  $\tilde{w}$  are the oscillating velocity components in  $i$ -direction and vertical direction, respectively.

The non-dimensional thickness  $\delta$  of the wave boundary layer is given by:

$$\delta = 0.09\alpha \left( \frac{A}{k_s} \right)^{0.82} \frac{k_s}{h} \quad (4.3a)$$

with:

$$\begin{aligned} \delta_{\max} &= 0.5 \\ \delta_{\min} &= \alpha \frac{ez_0}{h} \end{aligned} \quad (4.3b)$$

Here  $A$  is the wave orbital excursion parameter near the bed based on the root-mean-square wave height and peak period and  $z_0$  is given by  $k_s/33$  with  $k_s$  equal to the user-defined roughness height RKVAL. The factor  $\alpha$  represents the larger wave boundary layer thickness in irregular waves as compared to regular waves. When using  $\alpha = 1$ , Eq. (4.3a) reduces to the theoretical expression for monochromatic waves (see Fredsøe and Deigaard, 1992). Here  $\alpha$  is set equal to 20, on the basis of a comparison with measurements in irregular waves.

We make the assumption that the forcing  $R_i$  is dominated by a pressure gradient and that the depth-variation of  $R_i$  can be neglected:

$$R_i = \rho g h \frac{\partial h}{\partial x_i} \quad (4.4)$$

The *time-averaged* shear stress  $-\rho \tilde{u}_i \tilde{w}$  in Eq. (4.2b) results from the fact that in the wave boundary layer the horizontal and vertical velocities are not exactly 90 degrees out of phase. These stresses grow from zero at the bed to an asymptotic value  $-\rho(\tilde{u}_i \tilde{w})_\delta$  in which, from geometrical considerations  $\tilde{w}(\delta) = -\Delta\tau / \rho c$ . Here  $\Delta\tau$  is the increase of the instantaneous shear stress through the boundary layer. With the dissipation due to bottom friction given by  $D_f = \Delta\tau u(\delta)$  and assuming that the stress  $-\rho \tilde{u}_i \tilde{w}$  decreases linearly to zero across the wave boundary layer, the last term in Eq. (4.2b) is given by:

$$\frac{\partial}{\partial \sigma} \rho \tilde{u}_i \tilde{w} = -\frac{1}{\delta} \frac{D_f k_i}{\omega} \quad (4.5)$$

in which  $k_i$  is the wave number in  $i$ -direction and  $\omega$  is the angular frequency.

The dissipation due to bottom friction is computed as:

$$D_f = \frac{1}{2\sqrt{\pi}} \rho f_w u_{orb}^3 \quad (4.6)$$

where  $u_{orb}$  is the orbital velocity near the bed based on the root-mean-square wave height and the friction factor  $f_w$  is given by the following relationship (Soulsby, 1994):

$$f_w = 1.39 \left( \frac{A}{z_0} \right)^{-0.52} \quad (4.7)$$

$$f_{w,\max} = 0.3$$

Here  $A$  is the wave orbital excursion parameter near the bed based on the root-mean-square wave height and peak period and  $z_0$  is given by  $k_s/33$  with  $k_s$  equal to the user-defined roughness height RQUAL.

Since we assumed that the depth-variation of  $R_i$  can be neglected, integration of Eqs. (4.2a) and (4.2b) from the surface downwards yields:

$$\tau_i = \tau_{s,i} - R_i(1 - \sigma) \quad , \sigma > \delta \quad (4.8a)$$

$$\tau_i = \tau_{s,i} - R_i(1 - \sigma) + \frac{D_f k_i}{\omega} \frac{\delta - \sigma}{\delta} \quad , \sigma < \delta \quad (4.8b)$$

Here  $\tau_{s,i}$  is the known surface shear stress applied at mean water level, which accounts for wind stress and the shear stress introduced by the dissipation in the surface rollers. The formulation for the surface shear stress is described in Section 4.4.

The shear stress is related to the velocity gradients by:

$$\tau_i = \frac{\rho v_t}{h} \frac{\partial u_i}{\partial \sigma} \quad (4.9)$$

### 4.3 Vertical structure of eddy viscosity

For the computation of the mean current profile, we use an eddy viscosity model (zero equation turbulence model). The eddy viscosity is written as the product of a scale factor and a shape function, which are different for the boundary layer and middle layer respectively. The scale factors may vary with time and location along the profile. The shape functions are parabolic, such that the equations can be solved analytically, and are zero at  $\sigma = 0$ .

In the middle layer, the depth-averaged viscosity  $\bar{v}_t$  has been chosen as a scale factor yielding:

$$v_t = \phi_s \bar{v}_t \sigma (\sigma_s - \sigma) \quad , \sigma > \delta \quad (4.10)$$

where  $\sigma = z/h$ , the relative height above the bed and  $\delta$  is the scaled boundary layer thickness. The parameter  $\sigma_s$ , determining the shape of the viscosity distribution, is specified later on. The parameter  $\phi_s$  follows from the condition:

$$\int_0^1 \phi_s \sigma (\sigma_s - \sigma) d\sigma = 1 \quad (4.11)$$

Hence,

$$\phi_s = \frac{1}{\frac{1}{2} \sigma_s - \frac{1}{3}} \quad (4.12)$$

In the wave boundary layer, the eddy viscosity is increased relative to (4.10) to account for the increased turbulence in the boundary layer. This eddy viscosity increase is assumed to have a parabolic distribution throughout the boundary layer and is zero at  $\sigma = 0$  and  $\sigma = \delta$ . This yields for the eddy viscosity distribution in the boundary layer:

$$v_t = \phi_s \bar{v}_t \sigma (\sigma_s - \sigma) + \phi_b \bar{v}_{tb} \sigma (\delta - \sigma) \quad , \sigma < \delta \quad (4.13)$$

with  $\bar{v}_{tb}$  is the increased turbulence in the wave boundary layer.

Here the parameter  $\phi_b$  is determined by the condition:

$$\frac{1}{\delta} \int_0^{\delta} \phi_b \sigma (\delta - \sigma) d\sigma = 1 \quad (4.14)$$

and thus depends on the boundary layer thickness via:

$$\phi_b = \frac{6}{\delta^2} \quad (4.15)$$

It is convenient to write (4.13) in a similar form as Eq. (4.10):

$$v_t = (\phi v)_b \sigma (\sigma_b - \sigma) \quad , \sigma < \delta \quad (4.16)$$

with:

$$(\phi v)_b = \phi_s \bar{v}_t + \phi_b \bar{v}_{tb} \quad (4.17)$$

$$\sigma_b = \frac{\phi_s \bar{v}_t \sigma_s + \phi_b \bar{v}_{tb} \delta}{\phi_s \bar{v}_t + \phi_b \bar{v}_{tb}} \quad (4.18)$$

The definition of the  $\sigma$ -parameters is illustrated in the Figure 2.2. Note that this sketch of the shape of the eddy viscosity is a tentative one; the resulting eddy viscosity distribution strongly depends on the relative magnitudes of  $\delta$ ,  $\sigma_s$ ,  $\bar{v}_{tb}$  and  $\bar{v}_t$ .

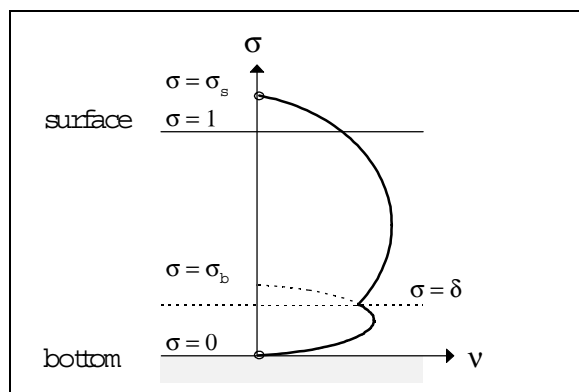


Figure 2.2 Definition of  $\sigma$ -parameters

## 4.4 Integration of velocity profile

### Analytical solution

We can now obtain the velocity profile by integrating Eq. (4.9); by integrating once more, we get the depth-mean velocity. A parabolic eddy viscosity has been chosen (see Eqs. 4.10 and 4.16), such that both integrations can be carried out analytically and yield relatively simple, logarithmic expressions. In Appendix A, details of this integration are given.

The first integration yields expressions for the current profile in the boundary layer (Eq. A.5) and in the middle layer (Eq. A.8). In these equations coefficients occur in terms of the the

depth-independent forcing  $R_i$ , the known surface shear stress  $\tau_{s,i}$  (see below for the computation of  $\tau_{s,i}$ ) and known streaming term  $(D_f k_i)/\omega$  (see Section 4.2).

The second integration results in a direct relationship between the depth-mean velocity  $\bar{u}_i$ , the depth-independent forcing  $R_i$ , the known surface shear stress  $\tau_{s,i}$  and known streaming term  $(D_f k_i)/\omega$  (see also Appendix A, Eq. (A.14)):

$$\bar{u}_i = (H_b + H - G_b - G)R_i + (G_b + G)\tau_{s,i} + \left(G_b - \frac{H_b}{\delta}\right)\left(\frac{D_f k_i}{\omega}\right) \quad (4.19)$$

When we apply the expressions to obtain the cross-shore current profile, the mean current is known via the condition that the net mean flow in the middle and bottom layer must compensate for the mass flux in the surface layer due to propagating and breaking waves. The unknown forcing (pressure gradient)  $R_x$  is solved from the depth-averaged expression (4.19). Having determined the forcing, the current profile can be computed directly using Eqs (A.5) and (A.8) for the current profile as given in Appendix A.

The coefficients in Eq. 4.19 and Eqs (A.5) and (A.8) depend on amongst others the depth-averaged viscosity  $\bar{\nu}_t$ . For the computation of  $\bar{\nu}_t$ , described in Section 4.5, the turbulence viscosity for a purely slope-driven current is needed, which itself depends on the surface slope in cross-shore and longshore direction. The surface slope in longshore direction is known from the tidal velocity as defined by the user (see further on in this section for the applied formulation). However, the cross-shore slope is only known when the unknown forcing (pressure gradient)  $R_x$  is solved from the depth-averaged expression (4.19) and Eq. 4.4. Therefore an iterative procedure is followed to obtain the forcing  $R_x$ .

In longshore direction, the forcing  $R_y$  follows directly from the known alongshore surface slope. With the forcing  $R_y$  and the depth-averaged viscosity known, the depth-mean current and the current profile can be computed directly from Eq. (4.19) and the Eqs (A.5) and (A.8).

### Surface layer effective shear stress

In order to solve Eqs (4.19), the surface shear stress  $\tau_{s,i}$  with  $i = x$  or  $y$ , has to be computed. The wave-induced shear stress translates the momentum decay of the surface layer due to wave breaking to the lower layers and provides the boundary condition for the middle layer. To this wave-induced shear stress, a wind stress is added.

The shear stress in the direction of wave propagation, introduced by the surface roller, is given by:

$$\tau_{s,wave} = \frac{Diss}{c} \quad (4.20)$$

in which  $Diss$  is the dissipation of roller energy (see Eq. 3.10).

For the wind stress in the wind direction, the following relation is used:

$$\tau_{s,wind} = 1.9555 * 10^{-5} u^2 + 0.0024u - 0.0054 + \frac{0.007}{u} \quad (4.21)$$

in which  $u$  is the wind velocity.

### Mass flux and cross-shore mean velocity

The mass flux in the surface layer is assumed to consist of two parts, one due to the progressive character of the waves and the other due to the surface roller in breaking waves:

$$q_{drift} = q_{non-breaking} + q_{roller} = \frac{E}{c} + \frac{\rho A c}{T} = \frac{E + 2E_r}{c} \quad (4.22)$$

Here the first part of the right hand side is the mass flux for non-breaking waves and follows from Phillips (1977), whereas the second part accounts for the contribution to the mass of the surface roller (see also Eq. 3.9). The cross-shore depth-mean velocity in the lower layers, necessary for the computation of the cross-shore current profile, must compensate for the mass flux and is therefore given by:

$$\bar{u}_x = -\frac{q_{drift,x}}{h} = -\frac{q_{drift} \cos \theta}{h} \quad (4.23)$$

### Longshore slope

In order to compute the forcing  $R_y$ , the alongshore surface slope must be derived from the user-defined depth-averaged tidal velocity at a certain reference depth.

We use the Chézy formulation which is based upon a logarithmic velocity profile along the complete water column:

$$\bar{v}_{tide} = C \sqrt{h \frac{\partial h}{\partial y}} \quad (4.24)$$

with  $C = 18 \log \frac{12h}{k_s}$

For the roughness height  $k_s$  in Eq. (4.24) the user-defined roughness (RKVAL) is used.

## 4.5 Specification of eddy viscosity distribution

In order to fully define the eddy viscosity distribution the following parameters have to be specified:

- the depth-averaged eddy viscosity  $\bar{\nu}_t$  for a combination of turbulence generated by slope-driven currents, wave-breaking and wind;
- the parameter  $\sigma_s$  for which the combined eddy viscosity profile is zero;

- the increased turbulence  $\bar{v}_{tb}$  in the wave boundary layer;
- the boundary layer thickness

These aspects will be specified in the following. First,  $\sigma_s$  and  $\bar{v}_t$  are presented for the situation of a purely slope-driven current, a purely wind-driven current, and turbulence generated purely by wave breaking respectively. Consequently, these results are combined to find  $\sigma_s$  and  $\bar{v}_t$  for the situation of turbulence generated by the combination of these sources. Finally, the relations for the increased turbulence  $\bar{v}_{tb}$  in the wave boundary layer and the boundary layer thickness are given.

### Depth-averaged turbulence viscosity for purely slope-driven current

For purely slope-driven currents, the distribution of the eddy viscosity is parabolic, and zero at  $\sigma = 0$  and  $\sigma = 1$ . This leads to  $\sigma_s = 1$  and with Eq. (4.12) to  $\varphi_s = 6$ .

Near the bottom, the velocity varies linearly with distance from the bed, with a gradient:

$$\frac{\partial u}{\partial \sigma} = \frac{u_*}{\kappa e \sigma_0} \quad (4.25)$$

For a slope-driven current with surface slope  $s_b$ , we have near the bed (see Eq. (A.4a)):

$$\frac{\partial u_i}{\partial \sigma} = A \left( \frac{B_i}{\sigma_s \sigma} + \frac{B_i / \sigma_s + C_i}{\sigma_s - \sigma} \right) = \frac{h}{\rho \phi_s \bar{v}_t} \left( \frac{-\rho g h s_b}{\sigma_s \sigma} \right) = \frac{h}{6 \rho \bar{v}_t} \frac{\tau_b}{e \sigma_0} \quad (4.26)$$

So, with  $\tau_b = \rho u_*^2$ :

$$\frac{u_*}{\kappa e \sigma_0} = \frac{h}{6 \bar{v}_t} \frac{u_*^2}{e \sigma_0} \quad (4.27)$$

The depth-averaged viscosity is now expressed as:

$$\bar{v}_{t,1} = \frac{1}{6} \kappa h \sqrt{g h |s|} \quad (4.28)$$

### Depth-averaged turbulence viscosity for wind-driven current

In the case of purely wind-driven current, it is unlikely that the viscosity goes to zero near the surface; rather, a maximum is expected there. We model this by assuming a half-parabolic distribution, with  $\sigma_s = 2$  and hence  $\varphi_s = 1.5$

Near the bottom, the velocity again varies linearly with distance from the bed:

$$\frac{\partial u}{\partial \sigma} = \frac{u_*}{\kappa e \sigma_0} \quad (4.29)$$

For wind-driven current, we have near the bed:

$$\frac{\partial u_i}{\partial \sigma} = A \left( \frac{B_i}{\sigma_s \sigma} + \frac{B_i / \sigma_s + C_i}{\sigma_s - \sigma} \right) = \frac{h}{\rho \phi_s \bar{v}_t} \left( \frac{\tau_{s,i}}{\sigma_s \sigma} \right) = \frac{h}{\frac{3}{2} \rho \bar{v}_t} \frac{\tau_{s,i}}{2e\sigma_0} \quad (4.30)$$

So:

$$\frac{u_*}{\kappa e \sigma_0} = \frac{h}{3 \bar{v}_t} \frac{u_*^2}{e \sigma_0} \quad (4.31)$$

The depth-averaged viscosity is now expressed as:

$$\bar{v}_{t,2} = \frac{1}{3} \kappa h \sqrt{\frac{|\tau_s|}{\rho}} \quad (4.32)$$

### Depth-averaged turbulence viscosity generated by wave breaking

The depth-averaged turbulence viscosity due to wave breaking is modelled according to Battjes (1975) as:

$$\bar{v}_{t,3} = \alpha_w \left( \frac{Diss}{\rho} \right)^{1/3} L \quad (4.33)$$

where  $\alpha_w$  is a coefficient and  $L$  is a typical length scale. Validation studies (LIP Delta Flume Experiment, LIP Shear Wave Experiment) indicate that choosing  $L = H_{rms}$  in combination within  $\alpha_w$  in the range of 0.05-0.10 leads to optimum results. The coefficient  $\alpha_w$  has to be specified by the user (FCVISC)

The distribution over the depth of the breaking-induced turbulence is assumed to be similar to that induced by wind stress ( $\sigma_s = 2$  and hence  $\phi_s = 1.5$ )

### Combination of turbulence viscosity from different sources

In the case that we have turbulence generated by different sources, a zero-equation turbulence model cannot be derived rigorously. We therefore have to choose a reasonable approximation, which meets a number of constraints:

- the combined viscosity profile must reduce to all of the above mentioned limit cases;
- given that the length scales must be similar for the processes mentioned, it seems reasonable to add turbulence energy from different sources. For the viscosity, since  $v_t = l\sqrt{k}$  with  $l$  the length scale of the turbulence and  $k$  the turbulent kinetic energy, we must therefore take the root-mean-square *rms* of the different viscosity components;

- to ensure that the equations can be solved analytically, the combined viscosity profile must be of the form described by Eq (4.10).

The second and third constraint cannot be met exactly simultaneously. However, a good approximation is taking the *rms* of the respective depth-averaged viscosity contributions instead of the *rms* of the viscosity distributions:

$$\bar{v}_t = \sqrt{\bar{v}_{t,current}^2 + \bar{v}_{t,wind}^2 + \bar{v}_{t,breaking}^2} \quad (4.34)$$

For a half-parabolic eddy viscosity distribution ( $\sigma_s = 2$  and hence  $\varphi_s = 1.5$ ) as assumed for both a wind-driven current and the turbulence generated by wave breaking, the viscosity at surface level is equal to 1.5 times the depth-averaged viscosity. With the viscosity at the surface in a purely slope driven current equal to zero, we approximate the viscosity at surface level by taking the *rms* of the depth-averaged contributions due to wind and wave breaking only:

$$v_{t,surface} = \frac{3}{2} \sqrt{\bar{v}_{t,wind}^2 + \bar{v}_{t,breaking}^2} \quad (4.35)$$

Herewith, the parabolic distribution is completely defined and the parameters  $\sigma_s$  and  $\varphi_s$  can be determined. We can write  $\sigma_s$  in terms of the combined depth-averaged viscosity and the viscosity at surface level:

$$\sigma_s = \frac{\bar{v}_t - \frac{1}{3} v_{t,surface}}{\bar{v}_t - \frac{1}{2} v_{t,surface}} \quad (4.36)$$

The parameter  $\varphi_s$  is given by Eq. (4.12).

### Increased turbulence in wave boundary layer

We relate the turbulence in the wave boundary layer to the wave orbital motion and the friction factor. The theoretical result for the wave friction factor for smooth laminar flow is:

$$f_w = \frac{2}{\sqrt{\frac{u_{orb}^2}{\omega \nu}}} \quad (4.37)$$

where  $\nu$  is the molecular viscosity.

Analogous to Eq (4.37), we can express the turbulence in the wave boundary layer as:

$$\begin{aligned} \bar{v}_{tb} &= \frac{c_f^2 u_{orb}^2}{\omega} \\ c_f &= \frac{f_w}{2} \end{aligned} \quad (4.38)$$

with  $f_w$  determined by Eq. (4.7), the orbital velocity  $u_{orb}$  based on the root-mean-square wave height and  $\omega$  the angular frequency corresponding to the peak wave period.

## 5 Near-bed orbital velocity

The model of the time-variation of the near-bed velocity (orbital motion) due to non-linear short waves and long waves related to wave groups is based on the concept described in Roelvink and Stive (1989). In short, this model consists of two parts:

- a contribution due to wave asymmetry which is computed using Rienecker and Fenton's (1981) method for monochromatic waves, where the mean wave energy and peak period are used as input for the case of random waves.
- a contribution due to bound long waves based on Sand (1982), and an empirical relationship for the phase of the bound long wave relative to the short wave envelope.

The bed load transport model of UNIBEST-TC requires a complete representative time-series of the near-bed velocity in order to compute bed load transport rates. Therefore a time-series is produced which has the same characteristics of asymmetry, long waves and amplitude modulation as a random wave field. The shortest time-series which can exhibit all of these features has a length of one short wave group, which is  $m$  waves long.

Starting point is a time series of the near-bed velocity in case of regular waves (including wave asymmetry), based on the Rienecker and Fenton model:

$$U_1(t) = \sum_{j=1}^n B_j \cos(j\omega t) \quad (5.1)$$

The amplitudes  $B_j$  are determined numerically (Rienecker and Fenton [1981]), such that the difference between the maximum and minimum velocity of the asymmetric waves equals the difference in case of monochromatic waves. Next this time series  $U_1(t)$  is modulated such that amplitude variation on the time scale of a wave group is taken into account. Finally the contribution due to bound long waves is included. This two-step approach will be outlined below.

### Wave group related amplitude modulation

By adding a second velocity time series which is slightly out of phase with the first according to (5.1), the amplitude modulation on the time scale of a wavegroup is introduced yielding a time series  $U_2(t)$ :

$$U_2(t) = \sum_{j=1}^n \cos(j\omega t) \varepsilon^j = \sum_{j=1}^n \cos(j\omega t) \left[ \frac{1}{2} (1 + \cos(\Delta\omega \cdot t)) \right]^j \quad (5.2)$$

where  $\Delta\omega = \omega/m$ ,  $m$  being the number of waves in one wavegroup which is set to 7 in UNIBEST-TC. The notation  $\varepsilon^j$  means "ε to the power  $j$ ".

Finally, the magnitude of  $U_2$  is corrected to  $U'_2$  in such a way, that the third moment of  $U'_2$  equals the third moment of  $U_1$ :

$$U'_2(t) = \left( \frac{\frac{1}{T} \int_0^T U_1^3 dt}{\frac{1}{mT} \int_0^{mT} U_2^3 dt} \right)^{1/3} U_2(t) \quad (5.3)$$

### Generation of a time series of a bound long wave

The second step implies the modelling of a bound long wave. In case of a random wave field the grouping of the short waves will generate bound long waves. The long wave velocity  $U_3$  is computed according to Roelvink and Stive (1989) who assume that the wave-group related features of a random wave field may be represented by a bichromatic wave train with equal amplitudes  $a_m$  and  $a_n$  respectively, and an accompanying bound long wave with amplitude  $\xi_a$ .

Values for  $a_m = a_n$  and  $\xi_a$  have to be found. In order to do so, the schematized wave train is required to have the same total surface variance:

$$m_0 \equiv \frac{1}{8} H_{rms}^2 = \frac{1}{2} a_n^2 + \frac{1}{2} a_m^2 + \frac{1}{2} \xi_a^2 \quad (5.4)$$

Furthermore, Sand (1982) estimates the long-wave amplitude resulting from two waves with equal amplitudes and frequencies of  $f_p$  and  $f_p + \Delta f$  respectively, as

$$\xi_a = -G_{nm} \frac{a_n a_m}{h} \quad (5.5)$$

where  $G_{nm}$  is a transfer function defined as

$$G_{nm} h = \frac{4\pi^2 D_n D_m \Delta k_{nm} h \cosh(\Delta k_{nm} h) + \frac{\Delta k_{nm} h (D_n - D_m) (k_n h D_m + k_m h D_n) \coth(\Delta k_{nm} h)}{2 D_n D_m} - 2\pi^2 (D_n - D_m)^2 \Delta k_{nm} h}{4\pi^2 (D_n - D_m)^2 \coth(\Delta k_{nm} h) - \Delta k_{nm} h}$$

In this expression,  $h$  is the water depth,  $\Delta k_{nm} = k_n - k_m$  and the parameters  $D_m$  and  $D_n$  are defined as  $\sqrt{h/gf_n}$  and  $\sqrt{h/gf_m}$  respectively.  $\Delta f_{nm}$  is the long wave frequency which reads

$$\Delta f_{nm} = f_n - f_m = \frac{\Delta \omega_{nm}}{2\pi} \quad (5.6)$$

Knowing the cross-shore variation of  $H_{rms}$  (as predicted by the wave propagation model), the amplitudes ( $a_n$ ,  $a_m$ ) and  $\xi_a$  of both the short wave envelope and the bound long-wave can be solved from (5.4) and (5.5). Using a long wave approximation (shallow water conditions), the velocity time series  $U_3(t)$  due to the long wave component is described by

$$U_3(t) = \hat{u}_l \cos(\omega_l t + \varphi) \quad (5.7)$$

where

$$\hat{u}_l = \xi_a \frac{\sqrt{gh}}{h} \quad (5.8)$$

and

$$\omega_l = \frac{\omega}{m} \quad (5.9)$$

In equation (5.7) the angle  $\varphi$  represents the phase shift between the long-wave and the short-wave envelope, which equals  $-\pi$  in the case of a complete bound long wave situation. In reality however, it appears that the cross-correlation coefficient is only slightly negative as long as we stay offshore from the surf zone, and that it changes into a positive correlation as we enter the surf zone. Roelvink and Stive (1989) conclude from flume experiments that the value of  $\cos(\varphi)$  correlates well with the ratio of local wave energy and the incident wave energy as expressed by the squared ratio of the local wave height over the deep water wave height  $(H_{rms}/H_{rms,0})^2$ . In UNIBEST-TC this empirical relationship is included via

$$\cos(\varphi) = C_r \left[ 1 - 2 \left( \frac{H_{rms}}{H_{rms,0}} \right)^2 \right] \quad (5.10)$$

where  $C_r$  is the correlation coefficient between wave envelope and long-wave surface variation (which equals 0.25, Roelvink and Stive, 1989) and  $H_{rms,0}$  the incoming wave height at the seaward boundary of the model.

Final step is the computation of the time series  $U_4(t)$  of the total orbital velocity, by simply adding the effects due the short-wave envelope and the bound long-wave:

$$U_4(t) = U_2'(t) + U_3(t) \quad (5.11)$$

## 6 Bed load transport

### 6.1 General

Separate transport formulations are used for bed load transport, bed load being that part of the load which is in more or less continuous contact with the bed, and suspended load transport. In this section, the applied quasi-steady bed load formulation is described. At small shear stresses the bed load transport formulation represents the transport occurring as individual particles moving over a rippled bed, while at higher shear stresses the formulation represents the sheet flow phenomenon where particles move as bed load in several layers over a plane bed.

### 6.2 Bed-load transport formulation

By correlation of various non-dimensional parameters using a range of datasets of sediment transport in oscillatory flow over horizontal beds, a generalized bed-load transport formula has been obtained by Ribberink (see Van Rijn et al., 1995). This formulation is used in UNIBEST-TC supplemented with corrections to account for slope effects on the transport.

The *non-dimensional* instantaneous bed-load transport vector  $\Phi_{bd}$ , defined as the ratio of bed-load transport rate  $q_b$  and the square-root of a parameter representing the specific under-water weight of sand grains, is given by

$$\Phi_{bd}(t) = \frac{q_b(t)}{\sqrt{\Delta g d_{50}^3}} = 9.1 \frac{\beta_s}{(1-p)} \left\{ |\theta'(t)| - \theta_c \right\}^{1.8} \frac{\theta'(t)}{|\theta'(t)|} \quad (6.1)$$

with:

$q_b$	=	bed-load transport rate in volume per unit time and width <i>including pores</i>
$d_{50}$	=	median grain diameter
$\Delta$	=	relative density = $(\rho_s - \rho)/\rho$
$\rho_s$	=	density of sediment = 2650 kg/m <sup>3</sup>
$\rho$	=	density of water
$p$	=	porosity of the sediment = 0.4
$g$	=	gravity acceleration
$\theta'$	=	dimensionless effective shear stress
$\theta_{cr}$	=	dimensionless critical shear stress
$\beta_s$	=	slope factor

Note that the computed transport rates include the pores and that for the porosity a constant value of 0.4 is taken. The water density is determined from the following expression as a function of water temperature  $Te$  and salinity  $Sa$  (Van Rijn, 1993):

$$\begin{aligned}\rho_w &= 1000 + 1.455 Cl - 0.0065(Te - 4 + 0.4Cl)^2; \\ Cl &= \frac{Sa - 0.03}{1.805}\end{aligned}\quad (6.2)$$

### Bed shear stress

The parameter  $\theta'(t)$  is the instantaneous dimensionless effective shear stress due to currents and waves:

$$\theta' = \frac{\tau'_b}{(\rho_s - \rho)gd_{50}} \quad (6.3)$$

and represents the *sediment forcing* as the ratio of the flow drag-force *on the grains* and the under-water weight of grains. The effective bed-shear stress  $\tau'_b$  is that part of the total bed shear stress which is transferred directly to the grains in the bed as skin friction. The form drag induced by *bed forms* is not effective in relation to bed load transportation.

For the computation of  $\theta'(t)$  a quadratic friction law is applied using intra-wave near-bed velocities of the combined wave-current motion and a weighed friction factor  $f'_{cw}$ .

$$\theta'(t) = \frac{\frac{1}{2} \rho f'_{cw} |u_b(t)| u_b(t)}{(\rho_s - \rho)gd_{50}} \quad (6.4)$$

in which  $u_b$  is the time-dependent (intra-wave) near-bottom horizontal velocity vector of the combined wave-current motion at the top of the wave boundary layer ( $z = \delta$ ). This vector is computed in UNIBEST-TC as the sum of the near-bed oscillating velocity signal (see Chapter 5) and the time-averaged velocity at 1 cm from the bed (see Chapter 4).

The computation of the bed shear stress and the wave-current friction factor is described in more detail in Chapter 9.

### Slope correction to bed load transport rates

In the case of a sloping bed not only the effects of slope to the initiation of motion (see below) have to be taken into account, but the transport directly induced by gravity as well when the grains have been set in motion. For that reason, the Bagnold parameter  $\beta_s$  (see also Eq. 6.1) is introduced which increases the transport rates in case of downslope transport and decreases the transport rates in case of upslope transport:

$$\beta_s = \left( 1 + \frac{\frac{dz_b}{ds}}{\tan \varphi} \right)^{-1} = \frac{\tan \varphi}{\tan \varphi + \frac{dz_b}{ds}} \quad (6.5)$$

with the slope:

$$\frac{dz_b}{ds} = \frac{u_{bx}}{|u_b|} \frac{dz_{bx}}{dx} \quad (6.6)$$

and  $\varphi$  the angle of repose, which may differ from the natural angle of repose. In UNIBEST-TC the angle of repose is a function of the cross-shore distance and is specified by the user (see Chapter 3). It should be remarked that this formulation is only valid for:

$$\left| \frac{dz_b}{ds} \right| < \tan \varphi \quad (6.7)$$

limiting the maximum slope of the bed which can be used in simulations.

Note that in UNIBEST-TC the slope in longshore direction is zero by definition.

### Initiation of motion

The parameter  $\theta_{cr}$  is the non-dimensional critical shear stress, representing the threshold of motion of sand grains. This threshold parameter is calculated according to the classical Shields curve as modelled by Van Rijn (1993) as a function of the non-dimensional grain size  $D_*$ . In this way, no iteration is necessary to obtain the critical shear stress, as would be the case when applying the classical Shields curve. In addition, the threshold parameter is corrected to account for the the effect of bed slope  $\alpha$  to the threshold of motion. Therefore,

$$\theta_{cr} = f(D_*, \alpha) \quad (6.8)$$

with

$$D_* = d_{50} \left( \frac{g\Delta}{\nu^2} \right)^{1/3} \quad (6.9)$$

with  $\nu$  is the kinematic viscosity of water (Van Rijn, 1993):

$$\nu = \frac{4 \cdot 10^{-5}}{20 + Te} \quad (6.10)$$

We follow Van Rijn (1993) who represents the Shields curve as follows:

$$\begin{aligned} \theta_{cr} &= 0.24 D_*^{-1} & , & & 1 < D_* \leq 4 \\ \theta_{cr} &= 0.14 D_*^{-0.64} & , & & 4 < D_* \leq 10 \\ \theta_{cr} &= 0.04 D_*^{-0.1} & , & & 10 < D_* \leq 20 \\ \theta_{cr} &= 0.013 D_*^{0.29} & , & & 20 < D_* \leq 150 \\ \theta_{cr} &= 0.055 D_* & , & & 150 < D_* \end{aligned} \quad (6.11)$$

This representation of the Shields curve is applied in the suspended load and the bed load module to represent the time-averaged and intra-wave threshold parameter respectively. Only in the bed load formulation a slope correction is applied to the critical shear stress.

### Slope correction to threshold parameter in bed load formulation

The threshold criterion (Eq. 6.11) in the bed load formula is adapted using the Schoklitsch factor to take account of the effect of bed slope on the initiation of motion:

$$\theta_{cr,slope} = \frac{\sin\left(\varphi + \arctan\left(\frac{dz_b}{ds}\right)\right)}{\sin\varphi} \theta_{cr} \quad (6.12)$$

with  $\theta_{cr}$  according to Eq. (6.11) and the bottom slope according to Eq. (6.6). This formulation results in an increase of the critical shear stress for upslope movement and an decrease of the critical shear stress for downslope movement.

As in the case of the transport rate correction (Eq. (6.5)), the threshold criterion with slope correction is only valid for:

$$\left|\frac{dz_b}{ds}\right| < \tan\varphi \quad (6.13)$$

### Time-averaged cross- and longshore bed load transport rates

The instantaneous cross- and longshore transport components are obtained from:

$$\begin{aligned} q_{bx} &= \frac{u_{bx}}{|u_b|} |q_b| \\ q_{by} &= \frac{u_{by}}{|u_b|} |q_b| \end{aligned} \quad (6.14)$$

in which  $u_b$  and  $q_b$  are respectively the time-dependent (intra-wave) near-bottom horizontal velocity vector and the bed-load transport vector of the combined wave-current motion.

The net wave-averaged bed-load transport rate is obtained by averaging of the time-dependent transport vector  $q_b(t) = (q_{bx}, q_{by})$  over the duration of the imposed near bottom velocity time series

## 7 Suspended load transport

### 7.1 General

The suspended sediment transport rate ( $q_s$ ) can be computed from the vertical distribution of fluid velocities and sediment concentrations, as follows:

$$q_s = \int_a^{h+\eta} VCdz \quad (7.1)$$

in which:

- $V$  = local instantaneous fluid velocity at height  $z$  above bed (m/s)
- $C$  = local instantaneous sediment concentration at height  $z$  above bed ( $\text{kg/m}^3$ )
- $h$  = water depth (to mean surface level), (m)
- $\eta$  = water surface elevation (m)
- $a$  = thickness of bed-load layer (m)

Defining:  $V = v + \tilde{v}$  and  $C = c + \tilde{c}$  (7.2)

in which:

- $v$  = time and space-averaged fluid velocity at height  $z$  (m/s)
- $c$  = time and space-averaged concentration at height  $z$  ( $\text{kg/m}^3$ )
- $\tilde{v}$  = oscillating fluid component (including turbulent component), (m/s)
- $\tilde{c}$  = oscillating concentration component (including turbulent component), ( $\text{kg/m}^3$ )

Substituting Eq. (7.2) in Eq. (7.1) and averaging over time and space yields:

$$\bar{q}_s = \int_a^h v c dz + \int_a^h \overline{\tilde{v}\tilde{c}} dz = \bar{q}_{s,c} + \bar{q}_{s,w} \quad (7.3)$$

in which:

$$\bar{q}_s = \int_a^h v c dz \quad \text{time-averaged current-related sediment transport rate (kg/sm)}$$

$$\bar{q}_{s,w} = \int_a^h \overline{\tilde{v}\tilde{c}} dz \quad \text{time-averaged wave-related sediment transport rate (kg/sm)}$$

The current-related suspended sediment transport is defined as the transport of sediment particles by the time-averaged (mean) current velocities (longshore currents, rip currents, undertow currents). The current velocities and the sediment concentrations are affected by the

wave motion. It is known that the wave motion reduces the current velocities near the bed and strongly increases the near-bed concentrations due to its stirring action. The wave-related suspended sediment transport is defined as the transport of sediment particles by the oscillating fluid components (cross-shore orbital motion).

## 7.2 Suspended load transport formulation

In UNIBEST-TC the wave-related suspended sediment transport is assumed to be small as compared to the current-related suspended sediment transport. The suspended load transport in volume per unit time and width ( $\text{m}^2/\text{s}$ ) *inclusive of pores* is therefore computed as:

$$q_{s,c} = \frac{\int_0^h v c \, dz}{(1-p)\rho_s} \quad (7.4)$$

with  $v$  is the time-mean velocity profile computed according to Chapter 4 and  $c$  is the time-mean concentration profile. The factor  $p$  is the porosity and is set equal to 0.4. The procedure for computation of the concentration profile is described in the following section.

## 8 Time averaged concentration profile

### 8.1 Convection-diffusion equation

Usually, the time-averaged convection-diffusion equation is applied to compute the equilibrium concentration profile in steady flow. This equation reads:

$$w_{s,m} \cdot c + \varphi_d \varepsilon_{s,cw} \frac{dc}{dz} = 0 \quad (8.1)$$

in which:

$w_{s,m}$	=	fall velocity of suspended sediment in a fluid-sediment mixture (m/s)
$\varepsilon_{s,cw}$	=	sediment mixing coefficient for combined current and waves (m <sup>2</sup> /s)
$c$	=	time-averaged concentration at height $z$ above the bed (kg/m <sup>3</sup> )
$\varphi_d$	=	damping factor dependent on the concentration(-)

Here, it is assumed that Eq. (8.1) is also valid for wave-related mixing. The computation of the fall velocity  $w_{s,m}$  and the turbulence damping factor  $\varphi_d$  are dealt with in Section 8.2. The procedure for computation of the mixing coefficient  $\varepsilon_{s,cw}$  is described in Section 8.3.

The convection-diffusion equation is solved by numerical integration from a near-bed reference level  $a$  to the water surface. At the reference level a concentration-type boundary condition is used. This reference concentration is given in Section 8.4.

### 8.2 Sediment fall velocity and turbulence damping

#### Particle fall velocity

The fall velocity of a sediment particle is computed according to Van Rijn (1993):

$$\begin{aligned} w_s &= \frac{\Delta g d_s^2}{18\nu} & , & 1 \quad \mu m < d_s \leq 100 \quad \mu m \\ w_s &= \frac{10\nu}{d_s} \left[ \left( 1 + \frac{0.01\Delta g d_s^3}{\nu^2} \right)^2 - 1 \right] & , & 100 \quad \mu m < d_s \leq 1000 \quad \mu m \\ w_s &= 11(\Delta g d_s)^{0.5} & , & 1000 \quad \mu m < d_s \end{aligned} \quad (8.2)$$

Here  $d_s$  is the diameter of the suspended sediment, and is a user-defined property. Van Rijn (1987) concluded on the basis of measurements that  $d_s$  should be in the range of 60 to 100% of the diameter of the median bed material size  $d_{50}$ . The kinematic viscosity  $\nu$  is computed according to Eq. (6.10).

## Fall velocity in a mixture

In high concentration mixtures, the fall velocity of a single particle is reduced due to the presence of other particles. In order to account for this hindered settling effect, the fall velocity in a fluid-sediment mixture is determined as a function of the sediment concentration  $c$  ( $\text{kg}/\text{m}^3$ ) and the particle fall velocity  $w_s$ :

$$w_{s,m} = \left(1 - \frac{c}{\rho_s}\right)^5 w_s \quad (8.3)$$

## Damping factor

The damping factor  $\varphi_d$  represents the influence of the sediment particles on the turbulence structure of the fluid. This effect becomes increasingly important for high sediment concentrations which result in stratification and hence damping of turbulence. The following relation is used (see Van Rijn, 1993):

$$\varphi_d = 1 + \left(\frac{c}{c_0}\right)^{0.8} - 2 \left(\frac{c}{c_0}\right)^{0.4} \quad (8.4)$$

in which  $c_0$  is the maximum concentration and  $c$  is the actual concentration. The maximum volume concentration is set to 0.65 which amounts to a maximum concentration  $c_0$  of  $1.7 \cdot 10^3 \text{ kg}/\text{m}^3$ .

## 8.3 Sediment mixing coefficient

### General

Measurements in wave flumes show the presence of suspended sediment particles from the bed up to the water surface. The largest concentrations are found close to the bed where the diffusivity is large due to ripple-generated eddies. Further away from the bed the sediment concentrations decrease rapidly because the eddies dissolve rather rapidly travelling upwards.

Various researchers have tried to model the suspension process by introducing an effective wave-related sediment mixing coefficient  $\epsilon_{s,w,\text{bed}}$  (Van Rijn, 1993).

Based on analysis of measured concentration profiles, the following characteristics were observed (Van Rijn, 1993);

- approximately constant mixing coefficient  $\epsilon_{s,w,\text{bed}}$  in a layer ( $z \leq \delta_s$ ) near the bed,
- approximately constant mixing coefficient  $\epsilon_{s,w,\text{max}}$  in the upper half ( $z \geq 0.5 h$ ) of the water depth,
- approximately linear variation of the mixing coefficient for  $\delta_s < z < 0.5 h$ .

For the current mixing coefficient, a constant mixing is assumed in the upper half of the water column which decreases linearly to zero in the lower half of the column.

A sketch of the resulting shape of the mixing coefficients is given in the below figure:

For combined current and wave conditions the sediment mixing coefficient is modelled as:

$$\varepsilon_{s,cw} = \sqrt{(\varepsilon_{s,w})^2 + (\varepsilon_{s,c})^2} \quad (8.5)$$

in which:

$$\begin{array}{ll} \varepsilon_{s,w} & \text{wave-related mixing coefficient (m}^2/\text{s)} \\ \varepsilon_{s,c} & \text{current-related mixing coefficient (m}^2/\text{s)} \end{array}$$

### wave-related mixing

The mathematical formulation for the wave-related mixing coefficient reads:

$$z \leq \Delta_s \quad \varepsilon_{s,w} = \varepsilon_{s,w,bed} \quad (8.6a)$$

$$z \geq 0.5 h \quad \varepsilon_{s,w} = \varepsilon_{s,w,max} \quad (8.6b)$$

$$L_s < z < 0.5 h \quad \varepsilon_{s,w} = \varepsilon_{s,w,bed} + [\varepsilon_{s,w,max} - \varepsilon_{s,w,bed}] \left[ \frac{z - \delta_s}{0.5h - \delta_s} \right] \quad (8.6c)$$

Equation (8.6) is fully defined when the thickness  $\Delta_s$  of the near-bed sediment mixing layer, the mixing coefficient  $\varepsilon_{s,w,bed}$  in the near-bed layer and the mixing coefficient  $\varepsilon_{s,w,max}$  in the upper layer are known.

The thickness  $\Delta_s$  of the near-bed sediment mixing layer is modelled according to Kroon and Van Rijn (1993) who analysed concentration profiles measured in the surf and swash zone near the Dutch coast of Egmond. They found that the mixing effect of spilling and plunging breaking waves can be represented by increasing the mixing layer thickness and proposed the following relationship:

$$\frac{\delta_s}{h} = 0.3 \left( \frac{H_s}{h} \right)^{0.5}, \quad \text{with:} \quad (8.7)$$

$$\delta_{s,minimum} = 0.05 \text{ m}$$

$$\delta_{s,maximum} = 0.20 \text{ m}$$

where  $H_s$  is the significant wave height and  $h$  the water depth.

For the mixing coefficient in the near-bed layer the following expression is used:

$$\varepsilon_{s,w,bed} = \alpha_b \hat{U}_\delta \delta_s \quad (8.9)$$

in which  $\hat{U}_\delta$  is the peak value of near-bed orbital velocity based on the significant wave height and peak period and the empirical coefficient  $\alpha_b$  equal to  $0.004 D^*$  (see Eq. (6.9)).

The mixing coefficient in upper layer reads:

$$\varepsilon_{s,w,\max} = 0.035 \frac{H_s h}{T_p} \quad (8.10)$$

in which  $T_p$  is the peak period of spectrum. The maximum value for  $\varepsilon_{s,w,\max}$  is set to  $0.01 \text{ m}^2/\text{s}$ , while the minimum value for  $\varepsilon_{s,w,\max}$  is the value of  $\varepsilon_{s,w,\text{bed}}$ .

### Current-related mixing

The current-related mixing coefficient  $\varepsilon_{s,c}$  reads:

$$\begin{aligned} \varepsilon_{s,c} &= k\beta u_{*,c} z(1 - z/h) && \text{for } z < 0.5 h \\ \varepsilon_{s,c} &= 0.25\beta\kappa u_{*,c} h && \text{for } z \geq 0.5 h \end{aligned} \quad (8.11)$$

in which  $\kappa$  is the constant of Von Karman ( $\kappa = 0.4$ ), the coefficient  $\beta$  is the ratio between sediment and fluid mixing coefficient and  $u_{*,c}$  is the bed shear velocity.

The bed shear velocity  $u_{*,c}$  is given by:

$$u_{*,c} = \frac{\sqrt{g} \bar{v}}{C} \quad (8.12)$$

Here  $\bar{v}$  is the depth-averaged velocity vector and  $C$  is the Chézy coefficient given by:

$$C = 18 \log \left( \frac{12h}{k_{s,c}} \right) \quad (8.13)$$

in which  $k_{s,c}$  is the current-related bed-roughness height which is a user-defined property (RC).

The coefficient  $\beta$  is the ratio between sediment and fluid mixing coefficient and is represented by (see Van Rijn, 1993):

$$\beta = 1 + 2 \left( \frac{w}{u_{*,c}} \right)^2, \text{ with } \beta_{\max} = 1.5 \quad (8.14)$$

This equation results in values larger than unity, indicating that the effect of an increase of the sediment mixing coefficient with respect to the fluid mixing coefficient due to centrifugal forces causing the particles to be thrown outside the eddies is dominant over the decrease of

the sediment mixing coefficient due to a incomplete response of the particles to turbulent fluctuations.

## 8.4 Reference concentration near the bed

The reference concentration  $c_a$  ( in  $\text{kg/m}^3$ ) is given by:

$$c_a = 0.015 \rho_s \frac{d_{50}}{a} \frac{T^{1.5}}{D_*^{0.3}} \quad (8.15)$$

in which  $D_*$  is the dimensionless particle parameter (see Eq. (6.9)),  $T$  is the dimensionless bed-shear stress parameter and the reference level  $a$  is the thickness of bed-load layer.

The reference level  $a$  is given by the maximum value of the current-related roughness  $k_{s,c}$  and wave-related roughness  $k_{s,w}$ , which are both defined by the user in the input file (RC and RW repectively).

The bed shear stress parameter is defined as follows:

$$T = \frac{\tau'_{b,cw} - \tau_{b,cr}}{\tau_{b,cr}} \quad (8.16)$$

in which:

$$\begin{aligned} \tau'_{b,cw} &= \text{time-averaged effective bed-shear stress (N/m}^2\text{)} \\ \tau_{b,cr} &= \text{time-averaged critical bed-shear stress according to Shields (N/m}^2\text{)} \end{aligned}$$

The time-averaged critical shear stress is computed as:

$$\tau_{b,cr} = (\rho_s - \rho) g d_{50} \theta_{cr} \quad (8.17)$$

with  $\theta_{cr}$  according to Eq. (6.11). Note that no bed slope correction is applied to the critical shear stress, as opposed to the critical shear stress for the bed load formula.

The formulations for the time-averaged effective bed shear stress are dealt with in Chapter 9.

## 9 Bed shear stress formulations

### 9.1 Introduction

The general procedure for computation of the time-averaged and instantaneous bed shear is described in this Section 9.2. In addition, Sections 9.3 and 9.4 describe the way in which these formulae are applied in the suspended load and bed load module, respectively. As a result of the separate development of the bed load and suspended modules, now combined in UNIBEST-TC, the shear stress formulations in the two modules

### 9.2 General procedure for the bed shear stress

#### Bed shear stress due to waves

The bed shear stress  $\tau_{b,w}(t)$  due to waves alone is related to the wave friction coefficient  $f_w$  by:

$$\tau_{b,w}(t) = \frac{1}{2} \rho f_w |u_{orb,\delta}(t)| u_{orb,\delta}(t) \quad (9.1)$$

in which  $u_{orb,\delta}$  is the instantaneous oscillating velocity just outside the wave boundary layer.

The wave friction factor is assumed to be constant over the wave cycle and is modelled according to Swart (1974):

$$f_w = \exp \left[ -6 + 5.2 \left( \frac{\hat{A}_\delta}{k_{s,w}} \right)^{-0.19} \right] \quad (9.2)$$

$$f_{w,\max} = 0.3$$

with  $\hat{A}_\delta$  is the peak value of near-bed orbital excursion according to linear wave theory and based on the significant wave height and peak wave period. The wave-related bed roughness height  $k_{s,w}$  is slightly different in the bed load and suspended load module and will be discussed in Section 9.4 and 9.3 respectively.

The mean (time-averaged) value of the magnitude of the bed shear stress can be written as:

$$\langle |\tau_{b,w}| \rangle = \frac{1}{2} \rho f_w \langle u_{orb,\delta}^2(t) \rangle = \frac{1}{4} \rho f_w \hat{U}_\delta^2 \quad (9.3)$$

where  $\hat{U}_\delta$  is the peak value of near-bed orbital velocity according to linear wave theory and based on the significant wave height and peak wave period.

### Bed shear stress due to currents

The current-related bed shear stress in the presence of waves can be modelled by assuming a two-layer system for the current velocity  $v$ :

- logarithmic velocity profile affected by the form roughness  $k_s$  inside the near-bed mixing layer;
- logarithmic velocity profile affected by the apparent roughness  $k_a$  ( $k_a > k_s$  due to the influence of waves on the current profile) outside the near-bed mixing layer.

With the roughness height  $z_0$  defined by  $k/30$ , the expressions for rough turbulent flow  $v(z)$  are:

$$\begin{aligned}
 v(z) &= \bar{v} \frac{\ln\left(\frac{30z}{k_a}\right)}{-1 + \ln\left(\frac{30h}{k_a}\right)} && \text{for } z \geq \delta \\
 v(z) &= v(\delta) \frac{\ln\left(\frac{30z}{k_s}\right)}{\ln\left(\frac{30\delta}{k_s}\right)} && \text{for } z < \delta \\
 v(\delta) &= \bar{v} \frac{\ln\left(\frac{30\delta}{k_a}\right)}{-1 + \ln\left(\frac{30h}{k_a}\right)}
 \end{aligned} \tag{9.4}$$

where  $\bar{v}$  is the depth-averaged velocity vector and the thickness  $\delta$  of the near-bed sediment mixing layer is equal to 0.1 m. The minimum value of  $\delta$  is the apparent roughness height  $k_a/30$ .

The shear stress velocity (at  $z = ez_0 = ek_s/30 < \delta$ ) is then given by:

$$v_* = \kappa v(ez_0) = \bar{v} \frac{\kappa \ln\left(\frac{30\delta}{k_a}\right)}{\left(-1 + \ln\left(\frac{30h}{k_a}\right)\right) \ln\left(\frac{30\delta}{k_s}\right)} \tag{9.5}$$

The bed shear stress, defined at  $z = z_0$ , due to currents in the presence of waves then reads:

$$\tau_{b,c} = \bar{v}^2 \frac{\rho \kappa^2 \left[ \ln \left( \frac{30\delta}{k_a} \right) \right]^2}{\left( -1 + \ln \left( \frac{30h}{k_s} \right) \right)^2 \ln \left( \frac{30\delta}{k_s} \right)^2} \quad (9.6)$$

In the absence of waves and thus a logarithmic velocity profile along the complete water column the bed shear stress is equal to:

$$\tau_{b,c,no\ waves} = \bar{v}^2 \frac{\rho \kappa^2}{\left( -1 + \ln \left( \frac{30h}{k_s} \right) \right)^2} = \rho g \left( \frac{\bar{v}}{C} \right)^2 \quad (9.7)$$

with  $C = 18 \log \frac{12h}{k_s}$

This can also be written as:

$$\tau_{b,c,no\ waves} = \frac{1}{8} \rho f_c \bar{v}^2 \quad (9.8a)$$

with:

$$f_c = 0.24 \left[ \log \frac{12h}{k_s} \right]^{-2} \quad (9.8b)$$

Combining 9.6 and 9.8 gives for the bed shear stress due to currents in the presence of waves:

$$\tau_{b,c} = \frac{1}{8} \alpha_r \rho f_c \bar{v}^2;$$

with

$$\alpha_r = \frac{\left[ \ln \left( \frac{30\delta}{k_a} \right) \right]^2 \left[ -1 + \ln \left( \frac{30h}{k_s} \right) \right]^2}{\left[ \ln \left( \frac{30\delta}{k_s} \right) \right]^2 \left[ -1 + \ln \left( \frac{30h}{k_a} \right) \right]^2} \quad (9.9)$$

Instead of in terms of the depth-averaged velocity, the bed shear stress due to currents in the presence of waves can also be expressed in terms of the velocity at a level  $z$  above the wave boundary layer. We therefore substitute Eq. (9.4a) in Eq. 9.9. This yields with unchanged definition of the current friction factor  $f_c$ :

$$\tau_{b,c} = \frac{1}{8} \alpha(z) \rho f_c v(z)^2;$$

with

$$\alpha(z) = \left[ \frac{-1 + \ln\left(\frac{30h}{k_s}\right)}{\ln\left(\frac{30z}{k_s}\right)} \right]^2 \quad (9.10)$$

### Bed shear stress due to the combined wave-current motion

The time-averaged bed shear stress under combined wave current motion now becomes:

$$\tau_{b,cw} = \langle |\tau_{b,w}| \rangle + \tau_{b,c} \quad (9.11)$$

The time-averaged shear stress due to waves and the shear stress due to currents can be computed from Eqs. (9.3) and (9.9) or (9.10), respectively.

For the time-dependent bed shear stress a slightly different formulations is used for the case of combined waves and currents. We follow the approach as suggested by Grant and Madsen (1979) who assume that the bed shear stress can be expressed as a quadratic function of the *combined wave/current velocity*  $u_b(t)$  at some height  $z$  above the bed (above the wave boundary layer):

$$\tau_b(t) = \frac{1}{2} \rho f'_{cw} |u_b(t)| u_b(t) \quad (9.12)$$

Here  $f'_{cw}$  is a (skin) friction factor for the combined wave-current motion.

In principle the problem is 2DH since waves and currents may interact under an arbitrary angle. The bed-shear stress  $\tau_b$  and near-bed velocity  $u_b$  are vectors in the same direction with varying magnitudes and varying directions during the wave cycle.

The above mentioned quadratic friction law is used together with a formulation for the weighted friction coefficient for currents and waves  $f'_{cw}$ . Following van Rijn (1993) the wave-current friction factor  $f'_{cw}$  is computed from the (skin) friction factors for 'waves alone' and 'currents in the presence of waves', weighted linearly with the relative strength of the near-bed net current and oscillatory velocity amplitude.

$$f'_{cw} = \alpha f'_c + (1 - \alpha) f'_w \quad (9.13)$$

with:

$$\alpha = \frac{\langle u_b \rangle}{\langle u_b \rangle + \hat{U}} \quad (9.14)$$

in which  $\langle u_b \rangle$  is the time-averaged or mean current near-bed velocity at level  $z$  (but above the wave boundary layer) and  $\hat{U}$  is the velocity amplitude of the wave-induced oscillatory flow near the bed (without mean current)

### 9.3 Bed shear stress in suspended load model

The suspended load module requires the magnitude of the time-averaged bed shear stress in the combined wave-current motion in order to compute the reference concentration (see Eqs. (8.15) and (8.16)).

The bed shear stress due to the combination of waves and currents is computed as the sum of the bed shear stress due to waves and currents respectively (Eq. (9.11)). Equations (9.3) and (9.9) are used to obtain the bed shear stress due to waves and currents. The current friction factor and the wave friction factor are defined by Eq. (9.8b) and Eq. (9.2) respectively.

For the wave-related roughness height  $k_{s,w}$  in Eq. (9.2) the user-defined wave-related roughness (RW) is used. The current-related roughness height  $k_s$  in Eqs. (9.8) and (9.9) is equal to the user defined value (RC), while the apparent roughness  $k_a$  is computed using the following relationship (Van Rijn, 1993):

$$\begin{aligned} \frac{k_a}{k_s} &= \exp\left(\frac{\gamma \hat{U}_\delta}{\bar{v}}\right) \\ \left(\frac{\hat{U}_\delta}{\bar{v}}\right)_{\max} &= 5 \\ k_{a,\max} &= 10k_s \end{aligned} \quad (9.15)$$

where  $\hat{U}_\delta$  is the peak value of near-bed orbital velocity. The coefficient  $\gamma$  was found to depend on the angle between waves and currents  $\alpha$  (rad) and is given by:

$$\gamma = 0.8 + \alpha - 0.3\alpha^2 \quad (9.16)$$

The so obtained current- and wave-related bed shear stresses are *total* bed shear stresses, i.e. they have to be multiplied by efficiency factors to obtain the *effective* bed-shear stress  $\tau'_b$ . The efficiency factor for currents is given by:

$$\mu_c = \frac{f'_c}{f_c} \quad (9.17)$$

in which the grain-related  $f'_c$  is obtained from Eq. (9.8b) using  $k_s = 3d_{90}$  and  $f_c$  by using  $k_s =$  RC in Eq. (9.8b).

The efficiency factor for waves is given by (Van Rijn, 1993):

$$\mu_w = \frac{0.6}{D_*} \quad (9.18)$$

## 9.4 Bed shear stress in bed load model

The bed load module requires instantaneous shear stresses in the combined wave-current motion which are computed using Eqs. (9.12-14) using the mean and oscillatory velocity components just outside the wave boundary layer ( $z = \delta$ ). The necessary current- and wave-related friction factors in Eqs. (9.13) are computed by using Eqs. (9.8b) and (9.2) respectively. As in the suspended load module  $f_c$  is obtained by using  $k_s = RC$  in Eq. (9.8b).

As opposed to the procedure in the suspended load module, the grain-related friction factor  $f'_c$  in Eq. (9.17) is obtained from Eq. (9.8b) using  $k_s = 3d_{90}$  for  $\theta' < 1$  and  $k_s = 3\theta'd_{90}$  for  $\theta' > 1$ . This same grain-related roughness value is used for  $f_w$  in Eq. (9.2) instead of the user-defined wave-related roughness (RW). Therefore, the use of the wave-related efficiency factor is superfluous.

For the computation of the roughness height  $k_s$  in the sheet flow regime ( $\theta' > 1$ ) a mean bed-shear stress (or Shields parameter) is necessary, which itself is dependent on  $k_s$ . Therefore an iterative procedure is followed in which a mean bed-shear stress just outside the wave boundary layer ( $z = \delta$ ) is first estimated with input of the grain roughness  $k_s = 3d_{90}$  using Eqs. (9.11), (9.3) and (9.10) for the computation of the mean bed-shear stress. With this bed-shear stress a new estimate of  $k_s$  is obtained using  $k_s = 3\theta'd_{90}$  and the computation is repeated until the solution converges and changes less than 1% during the last iteration. Note that the current-related roughness height  $k_s$  used in Eq. (9.10) is set equal to the user defined value (RC).

## References

- Battjes, J.A. (1975). Modelling of turbulence in the surf zone. Proc. Symp. on Modelling Techniques, San Francisco, ASCE pp. 1050-1061.
- Battjes, J.A., and J.P.F.M. Janssen (1978). Energy loss and set-up due to breaking in random waves. Proc. 16th Int. Conf. on Coastal Eng., ASCE, pp. 569-587.
- Battjes, J.A., and M.J.F. Stive (1985). Calibration and verification of a dissipation model for random breaking waves. J. Geophys. Res., 90(C5): 9159-9167.
- DELFT HYDRAULICS, 1995. Yearly averaged sediment transport along the Dutch shore; upgrading of UNIBEST-TC, report H2129.
- Fredsøe, J. and R.Deigaard, 1992. Mechanics of coastal sediment transport. World Scientific, Singapore.
- Grant, W.D. and O.S. Madsen, 1979. Combined wave and current interaction with a rough bottom. J. Geophys. Res., 84(C4): 1797-1808.
- Nairn, R.B., J.A. Roelvink and H.N. Southgate, 1990. Transition zone width and implications for modelling surfzone hydrodynamics. Proceedings of the Int. Conf. Coastal Engineering Conference, Delft, The Netherlands, pp. 68-82.
- Phillips, O.M., 1977. Dynamics of the upper ocean. 2nd ed. Cambridge University Press. London.
- Reniers, A.J.H.M., J.A. Roelvink and D.J.R. Walstra, 1995. Validation study of UNIBEST-TC; validation against the LIP 11D experiment, Report H2130, DELFT HYDRAULICS.
- Rienecker, M.M. and J.D. Fenton (1981). A Fourier approximation method for steady water waves. J. Fluid Mech., vol. 104, pp. 119-137.
- Roelvink J.A. and M.J.F. Stive, 1989. Bar-generating cross-shore flow mechanisms on a beach. J. Geophys. Res., Vol. 94, no. C4, pp. 4785-4800.
- Roelvink J.A. and A.J.H.M. Reniers, 1994. Upgrading of a quasi-3D hydrodynamic model. Abstracts-in-depth, MAST G8-M overall workshop, Gregynog.
- Roelvink, J.A., Th.J.G.P. Meijer, K. Houwman, R. Bakker and R. Spanhoff, 1995: Field validation and application of a coastal profile model. Int. Proc. Coastal Dynamics 1995, pp. 818-828.
- Rijn, L.C. van, 1987. Mathematical Modelling of Morphological Processes in the Case of Suspended Sediment Transport. Thesis, Dep. of Fluid Mechanics, Delft University of Technology, Delft, The Netherlands.
- Rijn, L.C. van, 1993. Principles of sediment transport in rivers, estuaries and coastal seas. Aqua Publ. (The Netherlands).
- Rijn, L.C. van et al., 1995. Yearly-averaged sand transport at the 20 m and 8 m NAP depth contours of the JARKUS-profiles 14, 40, 76 and 103, Report H1887, DELFT HYDRAULICS.
- Sand, S.E., 1982. Long wave problems in laboratory models. J. Waterw. Port Coastal Ocean Div. Am. Soc. Civ. Eng., 108, pp. 492-503.
- Soulsby, R.L., 1994. Manual of marine sands. HR Wallingford Report No. SR 351.
- Stive, M.J.F. and H.G. Wind, 1986. Cross-shore mean flow in the surf zone. Coastal Eng., 10, pp. 325-340.
- Stive, M.J.F. and H.J. De Vriend, 1994. Shear stresses and mean flow in shoaling and breaking waves. Proceedings of the Int. Conf. Coastal Engineering Conference, Kobe, Japan, pp. 594-605.
- Svendsen, I.A., 1985. On the formulation of the cross-shore wave-current problem. Proc. Workshop "European Coastal Zones", Athens, pp 1.1-1.9.
- Swart, D.H., 1974. Offshore sediment transport and equilibrium beach profiles, DELFT HYDRAULICS, Publ. 131.
- Vriend, H.J. de and Stive, M.J.F., 1987. Quasi-3D modelling of nearshore currents. In: P.P.G. Dyke (ed), JONSMOD'86, Coastal Eng. 11, pp. 565-601.

## A Velocity profile

### Velocity gradient

Using the depth-integrated momentum balance (Eqs 4.8a and 4.8b for the wave boundary layer and middle layer respectively), the definition of the eddy viscosity (Eqs 4.10 and 4.16) and the relation between shear stress and velocity gradient (Eq. 4.9), the vertical velocity gradient can be written as:

$$\frac{\partial u_i}{\partial \sigma} = \frac{h}{\rho \phi_s \bar{v}_t} \left( \frac{(\tau_{s,i} - R_i) + R_i \sigma}{\sigma(\sigma_s - \sigma)} \right) \quad , \sigma > \delta \quad (\text{A.1a})$$

$$\frac{\partial u_i}{\partial \sigma} = \frac{h}{\rho(\phi v)_b} \left( \frac{\left( \tau_{s,i} - R_i + \frac{D_f k_i}{\omega} \right) + \left( R_i - \frac{D_f k_i}{\delta \omega} \right) \sigma}{\sigma(\sigma_b - \sigma)} \right) \quad , \sigma < \delta \quad (\text{A.1b})$$

Eqs (A.1) can be written in the following form:

$$\frac{\partial u_i}{\partial \sigma} = A \left( \frac{B_i + C_i \sigma}{\sigma(\sigma_s - \sigma)} \right) \quad , \sigma > \delta \quad (\text{A.2a})$$

$$\frac{\partial u_i}{\partial \sigma} = A_b \left( \frac{B_{b,i} + C_{b,i} \sigma}{\sigma(\sigma_b - \sigma)} \right) \quad , \sigma < \delta \quad (\text{A.2b})$$

where the coefficients are given by:

$$A = \frac{h}{\rho \phi_s \bar{v}_t}; \quad B_i = \tau_{s,i} - R_i; \quad C_i = R_i \quad (\text{A.3a})$$

$$A_b = \frac{h}{\rho(\phi v)_b}; \quad B_{b,i} = \tau_{s,i} - R_i + \frac{D_f k_i}{\omega}; \quad C_{b,i} = R_i - \frac{D_f k_i}{\delta \omega} \quad (\text{A.3b})$$

Eqs (A.2) can be alternatively written as:

$$\frac{\partial u_i}{\partial \sigma} = A \left( \frac{B_i}{\sigma_s \sigma} + \frac{B_i/\sigma_s + C_i}{\sigma_s - \sigma} \right) \quad , \sigma > \delta \quad (\text{A.4a})$$

$$\frac{\partial u_i}{\partial \sigma} = A_b \left( \frac{B_{b,i}}{\sigma_b \sigma} + \frac{B_{b,i}/\sigma_b + C_{b,i}}{\sigma_b - \sigma} \right) \quad , \sigma < \delta \quad (\text{A.4b})$$

### Wave boundary layer

Given that  $u_i = 0$  at  $\sigma = \sigma_0$ , the velocity in the bottom layer is now obtained by integration of Eq. (A.4b):

$$u_i = A_b \left( \frac{B_{b,i}}{\sigma_b} \ln \frac{\sigma}{\sigma_0} - \left( \frac{B_{b,i}}{\sigma_b} + C_{b,i} \right) \ln \frac{\sigma_b - \sigma}{\sigma_b - \sigma_0} \right) \quad , \sigma < \delta \quad (\text{A.5})$$

This equation is valid for  $\sigma > e\sigma_0$ ; below this level, a linear velocity decay towards the bottom is assumed.

The contribution of these velocity components in the bottom layer to the depth-integrated flow follows from integration of Eq. (A.5). When, for simplicity, the lower boundary is taken as  $\sigma = \sigma_0$ , this results in:

$$\begin{aligned} \int_{\sigma_0}^{\delta} u_i d\sigma &= \\ &= A_b \left( \frac{B_{b,i}}{\sigma_b} \left( \sigma \ln \frac{\sigma}{\sigma_0} - \sigma \right) + \left( \frac{B_{b,i}}{\sigma_b} + C_{b,i} \right) \left( (\sigma_b - \sigma) \ln \frac{\sigma_b - \sigma}{\sigma_b - \sigma_0} + \sigma \right) \right) \Bigg|_{\sigma_0}^{\delta} = \\ &= A_b \left( \frac{B_{b,i}}{\sigma_b} \left( \delta \ln \frac{\delta}{\sigma_0} - (\delta - \sigma_0) \right) + \left( \frac{B_{b,i}}{\sigma_b} + C_{b,i} \right) \left( (\sigma_b - \delta) \ln \frac{\sigma_b - \delta}{\sigma_b - \sigma_0} + (\delta - \sigma_0) \right) \right) = \\ &= \frac{A_b}{\sigma_b} \left( \delta \ln \frac{\delta}{\sigma_0} + (\sigma_b - \delta) \ln \frac{\sigma_b - \delta}{\sigma_b - \sigma_0} \right) B_{b,i} + A_b \left( (\sigma_b - \delta) \ln \frac{\sigma_b - \delta}{\sigma_b - \sigma_0} + (\delta - \sigma_0) \right) C_{b,i} \end{aligned} \quad (\text{A.6})$$

The velocity at the top of the bottom layer ( $z = \delta$ ) follows from Eq. (A.5):

$$\begin{aligned} u_{\delta,i} &= A_b \left( \frac{B_{b,i}}{\sigma_b} \ln \frac{\delta}{\sigma_0} - \left( \frac{B_{b,i}}{\sigma_b} + C_{b,i} \right) \ln \frac{\sigma_b - \delta}{\sigma_b - \sigma_0} \right) = \\ &= \frac{A_b}{\sigma_b} \left( \ln \frac{\delta}{\sigma_0} - \ln \frac{\sigma_b - \delta}{\sigma_b - \sigma_0} \right) B_{b,i} - A_b \left( \ln \frac{\sigma_b - \delta}{\sigma_b - \sigma_0} \right) C_{b,i} \end{aligned} \quad (\text{A.7})$$

### Middle layer

The velocity at the top of the wave boundary layer is the lower boundary condition for the middle layer. With  $u_{\delta,i}$  according to Eq. (A.7), the velocity in the middle layer is now obtained by integration of Eq. (A.4a):

$$u_i = u_{\delta,i} + A \left( \frac{B_i}{\sigma_s} \ln \frac{\sigma}{\delta} - \left( \frac{B_i}{\sigma_s} + C_i \right) \ln \frac{\sigma_s - \sigma}{\sigma_s - \delta} \right) \quad , \sigma > \delta \quad (\text{A.8})$$

The contribution of these velocity components in the middle layer to the depth-integrated flow follows from integration of Eq. (A.8):

$$\begin{aligned} \int_{\delta}^1 u_i d\sigma &= \\ &= u_{\delta,i}(1-\delta) + A \left( \frac{B_i}{\sigma_s} \left( \sigma \ln \frac{\sigma}{\delta} - \sigma \right) + \left( \frac{B_i}{\sigma_s} + C_i \right) \left( (\sigma_s - \sigma) \ln \frac{\sigma_s - \sigma}{\sigma_s - \delta} + \sigma \right) \right) \Big|_{\delta}^1 = \\ &= u_{\delta,i}(1-\delta) + A \left( \frac{B_i}{\sigma_s} \left( \ln \frac{1}{\delta} - (1-\delta) \right) + \left( \frac{B_i}{\sigma_s} + C_i \right) \left( (\sigma_s - 1) \ln \frac{\sigma_s - 1}{\sigma_s - \delta} + (1-\delta) \right) \right) = \\ &= u_{\delta,i}(1-\delta) + \frac{A}{\sigma_s} \left( \ln \frac{1}{\delta} + (\sigma_s - 1) \ln \frac{\sigma_s - 1}{\sigma_s - \delta} \right) B_i + A \left( (\sigma_s - 1) \ln \frac{\sigma_s - 1}{\sigma_s - \delta} + (1-\delta) \right) C_i \end{aligned} \quad (\text{A.9})$$

### Depth-mean velocity

The depth-mean velocity components are approximated by the integral of the velocity components from  $\sigma = \sigma_0$  to mean water level ( $\sigma = 1$ )<sup>1</sup>. This integral is approximated by summation of Eqs (A.6) and (A.9):

$$\begin{aligned} \bar{u}_i &\approx \frac{1}{1-\sigma_0} \int_{\sigma_0}^1 u_i d\sigma \approx \int_{\sigma_0}^1 u_i d\sigma = \int_{\sigma_0}^{\delta} u_i d\sigma + \int_{\delta}^1 u_i d\sigma = \\ &= \frac{A_b}{\sigma_b} \left( \delta \ln \frac{\delta}{\sigma_0} + (\sigma_b - \delta) \ln \frac{\sigma_b - \delta}{\sigma_b - \sigma_0} \right) B_{b,i} + \\ &+ A_b \left( (\sigma_b - \delta) \ln \frac{\sigma_b - \delta}{\sigma_b - \sigma_0} + (\delta - \sigma_0) \right) C_{b,i} + \\ &+ u_{\delta,i}(1-\delta) + \frac{A}{\sigma_s} \left( \ln \frac{1}{\delta} + (\sigma_s - 1) \ln \frac{\sigma_s - 1}{\sigma_s - \delta} \right) B_i + A \left( (\sigma_s - 1) \ln \frac{\sigma_s - 1}{\sigma_s - \delta} + (1-\delta) \right) C_i \end{aligned} \quad (\text{A.10})$$

<sup>1</sup> Formally, the integration should be carried out from  $\sigma = 0$  to wave trough level. For simplicity, we integrate the formulations from  $\sigma = \sigma_0$  to mean water level.

Using  $u_{\delta,i}$  according to Eq. (A.7), the depth-mean velocity components (A.10) can be written as:

$$\begin{aligned}\bar{u}_i &= \frac{A_b}{\sigma_b} \left( \ln \frac{\delta}{\sigma_0} + (\sigma_b - 1) \ln \frac{\sigma_b - \delta}{\sigma_b - \sigma_0} \right) B_{b,i} + \\ &+ A_b \left( (\sigma_b - 1) \ln \frac{\sigma_b - \delta}{\sigma_b - \sigma_0} + (\delta - \sigma_0) \right) C_{b,i} + \\ &+ \frac{A}{\sigma_s} \left( \ln \frac{1}{\delta} + (\sigma_s - 1) \ln \frac{\sigma_s - 1}{\sigma_s - \delta} \right) B_i + A \left( (\sigma_s - 1) \ln \frac{\sigma_s - 1}{\sigma_s - \delta} + (1 - \delta) \right) C_i\end{aligned}\quad (\text{A.11})$$

and thus:

$$\bar{u}_i = G_b B_{b,i} + H_b C_{b,i} + G B_i + H C_i \quad (\text{A.12})$$

with the coefficients given by:

$$\begin{aligned}G_b &= \frac{A_b}{\sigma_b} \left( \ln \frac{\delta}{\sigma_0} + (\sigma_b - 1) \ln \frac{\sigma_b - \delta}{\sigma_b - \sigma_0} \right) \\ H_b &= A_b \left( (\sigma_b - 1) \ln \frac{\sigma_b - \delta}{\sigma_b - \sigma_0} + (\delta - \sigma_0) \right) \\ G &= \frac{A}{\sigma_s} \left( \ln \frac{1}{\delta} + (\sigma_s - 1) \ln \frac{\sigma_s - 1}{\sigma_s - \delta} \right) \\ H &= A \left( (\sigma_s - 1) \ln \frac{\sigma_s - 1}{\sigma_s - \delta} + (1 - \delta) \right)\end{aligned}\quad (\text{A.13})$$

Using Eqs. (A.3), the depth-mean velocity  $\bar{u}_i$  (A.12) can be rewritten as a function of the the depth-independent forcing  $R_i$ , the known surface shear stress  $\tau_{s,i}$  and known streaming term  $(D_f k_i)/\omega$ :

$$\bar{u}_i = (H_b + H - G_b - G) R_i + (G_b + G) \tau_{s,i} + \left( G_b - \frac{H_b}{\delta} \right) \left( \frac{D_f k_i}{\omega} \right) \quad (\text{A.14})$$

By solving the forcing  $R_i$  from (A.14), the coefficients  $B_{b,i}$ ,  $C_{b,i}$ ,  $B_i$  and  $C_i$  are known from Eq. (A.3) and the vertical distribution of the velocity components in x- and y-direction can readily be computed from Eqs (A.5) and (A.8) for the wave boundary layer and middle layer respectively.

The procedure for solving Eq. (A.14) is slightly different for the cross-shore and longshore direction. In cross-shore direction, the equation is used to solve the unknown forcing (pressure gradient)  $R_x$  from the known mean cross-shore velocity (equal to the mass flux in the surface layer) and the known surface shear stress component  $\tau_{s,x}$ . In longshore direction, the forcing  $R_y$  follows directly from the known alongshore surface slope. With the forcing  $R_y$ ,

known, the depth-mean current and the current profile can be computed directly from Eq. (A.14). One is referred to Section 4.4 for more details concerning the computational procedure.